Journal of Cluster Science
https://doi.org/10.1007/s10876-020-01912-6

ORIGINAL PAPER

Physicochemical Characterization of PHBV Nanoparticles Functionalized with Multiple Bioactives Designed to be Theranostics for Lung Cancer

Paula Solar[1] · Natalia Herrera[2] · Diego Cea[1] · Sindy Devis[1] · Fernando Gonzalez-Nilo[3] · Natalia Juica[1] · Mabel Moreno[1] · Maria Nella Gai[4] · Ignacio Brescia[5] · Soledad Henríquez[1,6] · Luis Velasquez[1]

Received: 20 April 2020 / Accepted: 7 October 2020

Abstract

Lung cancer is a neoplasm associated with bacterial infections, main reason, to design a combined chemotherapy and antimicrobial treatment. Due to adverse drug reactions, we designed and synthetized polymer Poly(3-hydroxybutyrate-co-3-hydroxyvalerate) (PHBV) nanoparticles loaded with clarithromycin and paclitaxel and Superparamagnetic Iron Oxide Nanoparticles (SPION). Spherical nanoparticles with diameters ranging between 176 ± 19 and 222 ± 68 nm, hydrophilic and had a net negative surface charge were obtained. These nanoparticles can be lyophilized and resuspended in polar environments without affecting their physicochemical characteristics and maintaining their antibacterial activity. Both drugs interacted differently with the polymer, avoiding competition between them and facilitating the simultaneous encapsulation. The paclitaxel loaded in these nanoparticles remains almost completely encapsulated during the first 24 h under physiological conditions, allowing its accumulation and release in sites of high permeability and retention, such as tumors. In summary, these PHBV nanoparticles loaded with clarithromycin, paclitaxel and SPION are a promising drug delivery system for use in theranostics against lung cancer.

✉ Paula Solar
paula.solar@zonavirtual.uisek.cl

[1] Instituto de Investigación Interdisciplinar en Ciencias Biomédicas (I3CBSEK), Facultad de Ciencias de la Salud, Universidad SEK, Fernando Manterola 0789, Santiago, Providencia, Chile

[2] Facultad de Ciencias Químicas y Farmacéuticas, Universidad de Chile, Santiago, Chile

[3] Center for Bioinformatics and Integrative Biology, Facultad de Ciencias de La Vida, Universidad Andrés Bello, Santiago, Chile

[4] Departamento de Ciencias y Tecnología Farmacéutica, Facultad de Ciencias Químicas y Farmacéuticas, Universidad de Chile, Santiago, Chile

[5] Fundación Instituto de Investigación Austral, Puerto Varas, Chile

[6] Instituto de Investigaciones Materno Infantil (IDIMI), Facultad de Medicina, Universidad de Chile, Santiago, Chile

Published online: 21 October 2020

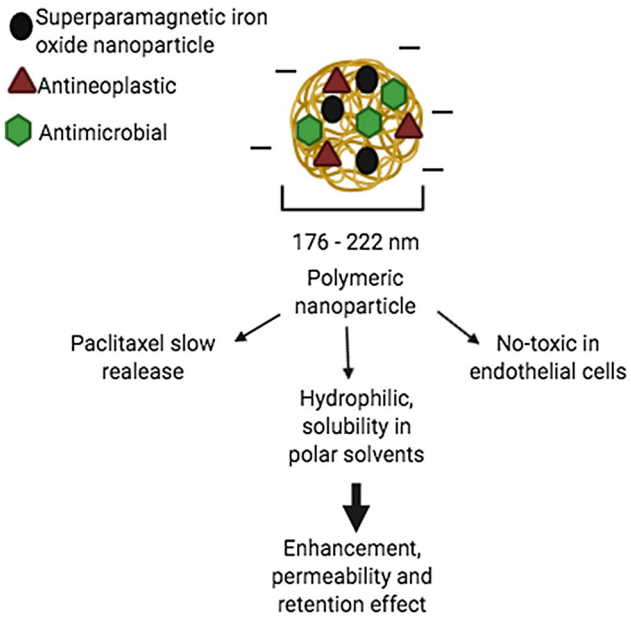

Keywords PHBV · Biopolymer nanoparticles · Clarithromycin · Paclitaxel · SPION

Introduction

Cancer is one of the leading causes of death worldwide according to the World Health Organization (WHO) and the National Cancer Institute (NIH) of the United States. Cancer causes 9.6 million deaths per year worldwide, of which 1.1 million are caused by lung cancer [1]. Lung cancer is an extremely aggressive neoplasm, and more than 50% of patients die before the first year after being diagnosed with lung cancer [2].

There are multiple causes and risk factors for lung cancer, such as smoking, genetic factors, contamination and bronchial pathologies [3]. The bronchial pathologies commonly associated with lung cancer are chronic bronchitis and asthma, both of which are associated with chronic infection with *Chlamydophila pneumoniae* (Cpn) [4]. Several antibiotics have activity against Cpn, of which the most clinically effective are azithromycin and clarithromycin, which have minimum inhibitory concentrations (MICs) of 0.2 ug/ml and 0.03 ug/ml, respectively [5].

Although clarithromycin has a much lower MIC than that of azithromycin, azithromycin has a longer half-life and greater tissue penetrability than those of clarithromycin [5]. One strategy to solve this, is to use nanopharmaceuticals have great potential as vehicles for the spatial and temporal release of bioactive and diagnostic compounds [6], allowing the use of drugs with low penetrability in tissues or the reduction of adverse drug reactions (ADRs).

Strategies to reduce ADRs would be to concentrate or localize the drug only in the target tissue and decrease the maximum plasma concentration of the drugs, which would limit its interaction with healthy tissue. A nanotechnological tool would allow strategies to be carried out, decreasing the plasma concentrations of drugs and simultaneously localizing them in the target tissue.

Conventional nanoparticulate systems have been used and designed to handle each aspect of pathology separately; however, from the theoretical point of view, some nanoparticles can exert multiple actions, leading to the production of multifunctional nanoparticles with therapeutic and diagnostic activity, which is defined as theranostics activity [7, 8].

Magnetic nanoparticles designed for theranostics can be simultaneously used as (i) contrast media for diagnostic and imaging follow-up, (ii) a therapy when used for drug delivery or for hyperthermia and (iii) a localized therapy, either active or passive. The management of pathologies through theranostics not only includes high specificity for the diagnosis and treatment of diseased cells but also includes the monitoring of the drug release process and its therapeutic efficacy [9]. The design of nanoparticles and the choice of their functionalization agents have direct

effects on the mode of action of nanoparticles at the diagnostic, monitoring and/or therapeutic levels.

Superparamagnetic Iron Oxide Nanoparticles (SPIONs) are among the most promising nanoparticles for use in theranostics due their physical characteristics, as they can be attracted by a magnetic field without aggregating to each other, which allows these nanoparticles to be localized in a specific area of the body with the use of a magnet [10, 11]. SPIONs have wide applications, among which the best known are the use of contrast media for magnetic resonance imaging (MRI), drug delivery and hyperthermia [12, 13]. Hyperthermia consists of a therapeutic procedure that increases the temperature of a region of the body to 40–43°C, which when carried out at the site of a tumor, is called oncological hyperthermia [14]. This treatment has been successful in both preclinical and clinical studies [15].

A polymer nanoparticle composed of SPIONs can be excellent carriers because in the presence of an alternating magnetic field, the SPIONs can be heated by raising the local temperature, which would lead to the elimination of tumor cells via hyperthermia and, at the same time, lead to increased degradation of the polymer, causing faster and more efficient release of the drug. On the other hand, the physical characteristics of SPIONs give them the ability to function as an excellent contrast medium for MRI, so hyperthermia can be performed by knowing the location of the nanoparticles in the body and using them to evaluate the effectiveness of the treatment [16, 17].

Several investigations have been carried out with SPIONs functionalized for potential use in theranostics. SPIONs loaded with doxorubicin shown to be able to serve for MRI and to have antitumor effects against lung cancer without systemic toxicity in C57BL6 mice [18]. SPIONs synthesized with doxorubicin and also conjugated with trastuzumab (Herceptin®) shown to be a good contrast medium for MRI and to have better inhibit tumor growth rate compared with free doxorubicin and Herceptin® [19].

Additionally, have been synthesized magnetic nanoparticles coated with polymer and conjugated with Pluronic® F127 bound to folic acid with potential for producing localized activity as well as for use in diagnosis and cancer therapy [20]. Folic acid was also used in conjunction with doxorubicin to functionalize SPIONs coated with polyethylene glycol (PEG) [21].

Multifunctional SPIONs covered with chitosan, PEG and conjugated with a monoclonal antibody against the Neu receptor (proto-oncogene that is overexpressed in approximately 30% of the most aggressive breast cancers resistant to chemotherapy) show highly specific binding to breast cancer and metastatic cells in the liver, lung and bone in a transgenic mouse model [22, 23].

Taking into account all this background we decided to design a nanoparticle with antineoplastic, superparamagnetic and antimicrobial activity against lung cancer. The antineoplastic and superparamagnetic activity would allow attacking the cancer cells, and the antibacterial activity would allow stopping a chronic Cpn infection or preventing it by acting as a prophylactic. For the antineoplastic activity we use paclitaxel, which is an antineoplastic widely used in the clinic. Superparamagnetic activity will be conferred by the use of SPION, and antimicrobial activity with the antibiotic clarithromycin.

In this work, we synthesized a novel polymeric Poly(3-hydroxybutyrate-co-3-hydroxyvalerate) (PHBV) nanoparticles functionalized with paclitaxel, clarithromycin and SPIONs for improving the solubility, permeability and retention of the encapsulated drugs. These nanoparticles would potentially allow favors their accumulation in tumors. These nanoparticles may be candidates for use in theranostics against lung cancer.

Methodology

Synthesis of Poly(3-hydroxybutyrate-co-3-hydroxyvalerate) (PHBV) Nanoparticles with Paclitaxel, Clarithromycin and SPIONs

Eight types of nanoparticles were synthesized: (1) empty PHBV nanoparticles (E), (2) PHBV nanoparticles with SPIONs (S), (3) PHBV nanoparticles with paclitaxel (T), (4) PHBV nanoparticles with clarithromycin (C), (5) PHBV nanoparticles with paclitaxel and clarithromycin (TC), (6) PHBV nanoparticles with clarithromycin and SPIONs (SC), (7) PHBV nanoparticles with paclitaxel and SPIONs (ST) and (8) PHBV nanoparticles with paclitaxel, clarithromycin and SPIONs (SCT). To carry out the synthesis of these nanoparticles, we used a double emulsion method modified from the method we reported previously [24, 25]. The first emulsion was carried out with 1 ml of PHBV with 12% PHV at a concentration of 3 mg/ml and 400 µL of the drugs to be encapsulated: 5 µM paclitaxel (p.a. $\geq$ 97%, Sigma) and 100 µg/ml clarithromycin (HPLC grade, Sigma) dissolved in dimethyl sulfoxide (DMSO) (p.a. $\geq$ 99.9%, Merck); both solutions were sonicated at 20% power for 1 min. For the second emulsion, 4 ml of 1% PVA was added (p.a. 98–99% PM 31.000–50.000, Sigma); then the mixture was sonicated for 1 min at 80% power, and the solvent was allowed to evaporate overnight with agitation at room temperature. Finally, the obtained nanoparticles were washed and collected in 1 ml of ultrapure water [24, 25].

Electron Microscopy

The morphology of the nanoparticles was determined from transmission electron microscopy (TEM) images using low-voltage electron microscopy (LVEM). For this purpose, a drop of nanoparticles was placed on an ultrathin Lacey carbon-coated 400-mesh copper grid and left to dry at room temperature for 10 min prior to image acquisition, ensuring no more than 1 min of exposure of the sample to the electron beam. Microscopy images were acquired using an LVEM5 electron microscope (Delong Instrument, Montreal, Quebec, Canada) with a voltage of 5 kV. The low voltage used allowed visualization of organic materials, omitting the staining procedure. Digital images were captured using a Retiga 4000R digital camera (QImaging, Inc., USA) [25].

Dynamic Light Scattering (DLS)

The size and Z potential of the nanoparticles were measured with a Malvern Zetasizer nano ZS®. The obtained nanoparticles were centrifuged and resuspended in 1 ml of ultrapure water. The measurements were performed using a reflectance of 0.33 [24, 25].

Contact Angle

Hydrophobicity was determined by contact angle measurement using a goniometer (OCA 15EC, Dataphysics). For this purpose, freeze-dried nanoparticles were placed on a film, and then, a drop of water was deposited on them. The image obtained from the drop of water was used to measure the contact angle between the nanoparticles and the drop, which indicated the degree of hydrophobicity of the sample. After depositing the drop of water on the sample, 1 photo per second was taken for 20 s to calculate the advance angle (AA), recoil angle (AR) and stationary angle (ASS) [29].

Determination of the Encapsulation Effectiveness

The encapsulation effectiveness of the drugs was determined by the extraction method previously described by Mao et al. [26]. Briefly, 10 mg of nanoparticles was dissolved in 2 ml of dichloromethane (DCM) (HPLC grade, Merck) and 5 ml of methanol (p.a. 99.9%, Merck) and left for 24 h at 37°C with shaking at 100 rpm. The concentration of the encapsulated drugs was measured by an ultra-performance liquid chromatography (UPLC) Acquity system (Waters, Milford, MA, USA) using a calibration curve. The encapsulation efficiency percentage (%EE) was calculated with the following equation [24–26]:

$$\%\mathrm{EE} = (\text{mg encapsulated} / \text{mg theoretical}) \times 100\%$$

Evaluation of Drug-Polymer Affinity

The Monte Carlo method was used to evaluate the affinity of the drugs to the PHBV polymer [27]. A conformational sampling algorithm based on a strategy using the Euler angle between two molecules, which contacted each other via their Van de Waals surfaces, was implemented. Force fields for the polymer and compounds were generated using HF/6-31G** quantum mechanics methods.

Drug Release Profile

A rapid equilibrium dialysis RED Device (Pierce, Thermo Scientific) certified dialysis system was used to measure the release of the encapsulated drugs. Seven milligrams of nanoparticles was dialyzed at 37°C with shaking against PBS (pH 7.4, Pierce, Thermo Scientific). The solution was extracted from the sampling chamber at 3 min and at 3, 7 and 28 h. To determine the release of paclitaxel, the supernatants were analyzed by HPLC [25]. Briefly, a 4.6 × 50 mm C18 column with a 5 µm particle size operated at room temperature was used. The mobile phase was acetonitrile/water 70/30 v/v at a flow rate of 1 ml/min.

Measurement of the Activity of the Nanoparticle Components

The activity of encapsulated clarithromycin (HPLC grade, Sigma) was measured using the Kirby-Bauer assay, which is better known as an antibiogram. The aim of this measurement was to determine whether the antibiotic remained active after being encapsulated in PHBV nanoparticles. *Neisseria gonorrhoeae* (Ngo strain P9-17) was used in the clarithromycin assay. Each Petri dish was inoculated with GC agar (BD) with 106 CFU of Ngo. The optical density was determined using a spectrophotometer (Synergy H1, Biotek) at a wavelength of 600 nm. Four milligrams of nanoparticles was loaded in each sensidisc, and 10 µg of free drug was used as a control. Ten micrograms of the antibiotic was used because this amount was within the range of the encapsulated antibiotic. The activity of encapsulated paclitaxel was not evaluated, as it has been previously evaluated for the same type of nanoparticle following the same synthesis protocol [25]. Additionally, the superparamagnetism of the nanoparticles was not evaluated because it has been shown that SPIONs in PHBV maintain their superparamagnetic activity [24].

In Vitro *Toxicity*

To determine the toxicity of nanoparticles, cell viability was determined quantitatively using alamar blue (alamarBlueTM cell viability reagent, Thermo Fisher Scientific), using the Eahy.926 cell line. Maintenance and expansion of the culture was carried out as recommended by ATCC using 10% fetal bovine serum IMDM medium [24, 25]. Briefly, to perform this Alamar Blue test and determine cytotoxicity in EA.hy926 cells, we first determined the number of cells capable of reducing an amount of Alamar Blue that was within the linear detection range of the equipment, using the manufacturer's suggested protocol. The experiment was conducted with 32,000 Eahy.926 cells that were cultured at 80% confluence for 24 h in IMDM (Hyclone) supplemented with 10% fetal bovine serum (FBS) in 96-well plates, followed by 24 h in serum-free medium. After this, Eahy.926 cells were cultured for 24 h under different treatment at 37°C and 5% CO2. The treatment consisted of 0.1, 1, 10 and 100 mg/mL nanoparticles in IMDM culture medium. The determinations were made in duplicate, for each of the synthesized nanoparticles, by performing three independent experiments. After incubation, treatment was removed and 110 µl of a solution with 100 µL of IMDM medium plus 10 µL of Alamar Blue were added. The cells were incubated for 3 h in darkness at 37 °C and 5% CO_2, and then the concentration of reduced Alamar Blue was measured by optical density in an ELISA reader (Synergy H1, Biotek) at 570 and 600 nm absorbance. The data obtained were plotted using the Graph pad Prism 5 program. The controls consisted of untreated cells, corresponding to 100% viability; a target control corresponding to cell-free medium, which was assigned 0% viability, and reduced 100% Alamar Blue. The result was expressed as a percentage of viability.

Statistical Analysis

The physicochemical characteristics of the nanoparticles are expressed as the mean ± standard deviation (SD) of 3 different samples in duplicate, measured three times each. In vitro analyses were analyzed by two-tailed ANOVA with a 95% confidence interval, and each nanoparticle was compared with each of the controls by the T-test followed by a paired assay.

Results

To physicochemically characterize PHBV nanoparticles with antineoplastic, bactericidal and superparamagnetic properties, we synthetized eight types of nanoparticles that differed in regard to their functionalizing molecules: (i) empty PHBV nanoparticles (E), (ii) PHBV nanoparticles functionalized with clarithromycin (C), (iii) PHBV nanoparticles functionalized with paclitaxel (T), (iv) PHBV nanoparticles functionalized with SPIONs (S), (v) PHBV nanoparticles functionalized with paclitaxel and clarithromycin (CT), (vi) PHBV nanoparticles functionalized with SPIONs and paclitaxel (ST), (vii) PHBV nanoparticles functionalized with SPIONs and clarithromycin (SC) and (viii) PHBV nanoparticles functionalized with SPIONs, paclitaxel and clarithromycin (SCT). For each category of synthesized nanoparticles, their size, polydispersity and z potential were evaluated by DLS. Table 1 show that all the evaluated nanoparticles have the appropriate dimensions, and the polydispersity indices (Pld) show that the synthesized nanoparticles have an adequate size distribution for biological use (≤ 0.20). On the other hand, the net surface charge (Z potential) of the nanoparticles is negative, indicating an adequate half-life in blood, without toxicity to endothelial cells via autophagy. The data show that the synthesized nanoparticles have an adequate size and surface charge to be able to be administered through an intravenous bolus and are candidates to have enhanced permeability and retention to allow them to accumulate in neoplastic tissues, according to the Nanotechnology Characterization Laboratory of the United States (NCL), in this research NCL assayed 130 different types of nanoparticles, and concluded that nanoparticles with negative surface charge, and size between 100 to 220 nm, and high solubility will has EPR effect [28].

To ensure that these nanoparticles have all the necessary characteristics of the desired in vivo behavior, it was necessary to measure their hydrophobicity, as shown in Table 2. Contact angle measurements above 90° correspond to hydrophobic materials, between 90° and 30° to hydrophilic materials and less than 30° to superhydrophilic materials [29]. The contact angles measured in the synthesized PHBV nanoparticles indicate that they correspond to hydrophilic materials. The data show that the synthesized nanoparticles have the ideal physicochemical characteristics of the desired behavior [30].

To evaluate the stability of the nanoparticles and their optimal storage conditions, the synthesized nanoparticles were lyophilized and stored at – 20 °C. The lyophilized nanoparticles used for the hydrophobicity measurement were resuspended in ultrapure water to measure their size, Z potential and polydispersity. The Table 3 show that lyophilized nanoparticles were reconstituted without any problems. Despite small variations in their size and Z potential, all the values were within the same range as newly synthesized nanoparticles.

The size and morphology of the synthesized nanoparticles were also evaluated by low voltage electron microscopy. These results corroborate the data obtained through

Table 1 Size, polydispersity and Z potential of synthesized nanoparticles

Nanoparticle	Diameter (nm) ± SD	Pdl ± SD	Zeta potential (mV) ± SD
E	220 ± 10	0.2 ± 0.0	− 10.8 ± 1.5
T	198 ± 14	0.1 ± 0.0	− 13.2 ± 1.2
C	215 ± 24	0.1 ± 0.0	− 11.2 ± 1.3
CT	201 ± 15	0.2 ± 0.0	− 13.4 ± 0.7
S	215 ± 4	0.2 ± 0.0	− 14.7 ± 1.2
SC	233 ± 4	0.2 ± 0.0	− 12.7 ± 0.2
ST	232 ± 19	0.2 ± 0.0	− 14.3 ± 1.0
SCT	215 ± 11	0.1 ± 0.0	− 17.7 ± 1.2

(E) Empty PHBV nanoparticles, (T) PHBV nanoparticles containing paclitaxel, (C) PHBV nanoparticles containing clarithromycin, (CT) PHBV nanoparticles containing clarithromycin and paclitaxel, (S) PHBV nanoparticles containing superparamagnetic iron oxide nanoparticles (SPIONs), (SC) PHBV nanoparticles containing SPIONs and clarithromycin, (ST) PHBV nanoparticles containing SPIONs and paclitaxel, and (SCT) PHBV nanoparticles containing SPIONs, clarithromycin and paclitaxel. PdL = polydispersity. Data were presented as mean ± SD (n = 3)

Table 2 Contact angle of synthesized nanoparticles

Nanoparticle	FA° ± SD	RA° ± SD	SSA° ± SD
E	84.9 ± 5.3	47.8 ± 9.2	66.4 ± 3.0
T	76.9 ± 4.7	43.4 ± 7.0	60.2 ± 1.2
C	77.4 ± 0.4	36.8 ± 3.8	57.1 ± 2.1
CT	66.5 ± 1.6	58.9 ± 3.2	51.3 ± 2.2
S	78.6 ± 12.9	49.2 ± 7.8	63.9 ± 10.3
SC	83.5 ± 0.5	77.0 ± 4.0	70.5 ± 1.2
ST	82.5 ± 3.2	43.9 ± 5.7	63.2 ± 2.1
SCT	80.1 ± 1.2	74.4 ± 3.6	68.6 ± 1.3

(FA) Forward angle, (RA) reverse angle and (SSA) stationary angle. (E) Empty PHBV nanoparticles, (T) PHBV nanoparticles containing paclitaxel, (C) PHBV nanoparticles containing clarithromycin, (CT) PHBV nanoparticles containing clarithromycin and paclitaxel, (S) PHBV nanoparticles containing superparamagnetic iron oxide nanoparticles (SPIONs), (SC) PHBV nanoparticles containing SPIONs and clarithromycin, (ST) PHBV nanoparticles containing SPIONs and paclitaxel, and (SCT) PHBV nanoparticles containing SPIONs, clarithromycin and paclitaxel. Data were presented as mean ± SD (n = 3)

DLS; we observed only one hydrodynamic diameter between 176 ± 19 nm and 222 ± 68 nm, which indicates with spherical nanoparticles. It was observed that nanoparticles containing clarithromycin had more electrodense points than those that did not contain this drug. Representative images are shown in Fig. 1.

After obtaining the physicochemical parameters of the synthesized nanoparticles, the effectiveness of drug encapsulation of the nanoparticles was measured in the presence and absence of SPIONs. These data are summarized in Table 4. The effectiveness of SPION encapsulation and their activity, was measured in previous research [24]. Briefly, we performed a hysteresis curve to ensure that SPIONs were encapsulated in the PHBV nanoparticles and maintained their physicochemical properties be making the PHBV nanoparticles superparamagnetic. On the other hand, the efficiency of the encapsulation (% EE) of paclitaxel decreases when encapsulated with SPIONs and also decreases when encapsulated with clarithromycin. There were no significant differences between both % EE. Even so, a significant decrease in the %EE of paclitaxel was expected, as both drugs are hydrophobic and compete for insertion into the polymeric matrix. However, clarithromycin alone has much lower encapsulation effectiveness than that of paclitaxel; however, the net amount of encapsulation is much higher because the amount of encapsulated clarithromycin is greater than that of paclitaxel (1.45 µg for paclitaxel and 15.05 µg for clarithromycin for 10 mg of nanoparticles). Although the physicochemical characteristics of nanoparticles with paclitaxel do not significantly differ from those of nanoparticles with clarithromycin, there are morphological differences, as seen in electron microscopy images by LVEM. Considering the morphological differences and the differences in %EE, the drug-polymer affinity was modeled using the Monte Carlo method. In this way, the structural elements that guide the gradual release of these molecules were identified.

The energy data for minimum interaction and the average energy between the compounds and the polymer are reported in the table of Fig. 2a, where the total interaction energy is indicated along with the energy components of the Van der Waals interaction and electrostatics that adopt the most stable conformation of the molecule with the polymer. It is observed that paclitaxel has the strongest interaction with the polymer, which, due to its structural characteristics, has an oxetane ring that maintains a strong van der Waals interaction with the polymer. As seen in Fig. 2b, c), both drugs have minimal energy

Table 3 Size, polydispersity and Z potential of lyophilized nanoparticles

Nanoparticle	Diameter (nm) ± SD	PdI ± SD	Zeta potential (mV) ± SD
E	219 ± 47	0.3 ± 0.0	− 13.0 ± 7.4
T	194 ± 53	0.2 ± 0.0	− 15.8 ± 6.1
C	195 ± 35	0.2 ± 0.0	− 12.2 ± 5.7
CT	176 ± 19	0.2 ± 0.1	− 16.9 ± 1.8
S	222 ± 68	0.2 ± 0.0	− 14.2 ± 0.3
SC	232 ± 35	0.2 ± 0.1	− 8.0 ± 10.1
ST	196 ± 27	0.2 ± 0.0	− 12.3 ± 2.8
SCT	202 ± 9	0.3 ± 0.1	− 14.0 ± 11.8

(E) Empty PHBV nanoparticles, (T) PHBV nanoparticles containing paclitaxel, (C) PHBV nanoparticles containing clarithromycin, (CT) PHBV nanoparticles containing clarithromycin and paclitaxel, (S) PHBV nanoparticles containing superparamagnetic iron oxide nanoparticles (SPIONs), (SC) PHBV nanoparticles containing SPIONs and clarithromycin, (ST) PHBV nanoparticles containing SPIONs and paclitaxel, and (SCT) PHBV nanoparticles containing SPIONs, clarithromycin and paclitaxel. Data were presented as mean ± SD (n = 3)

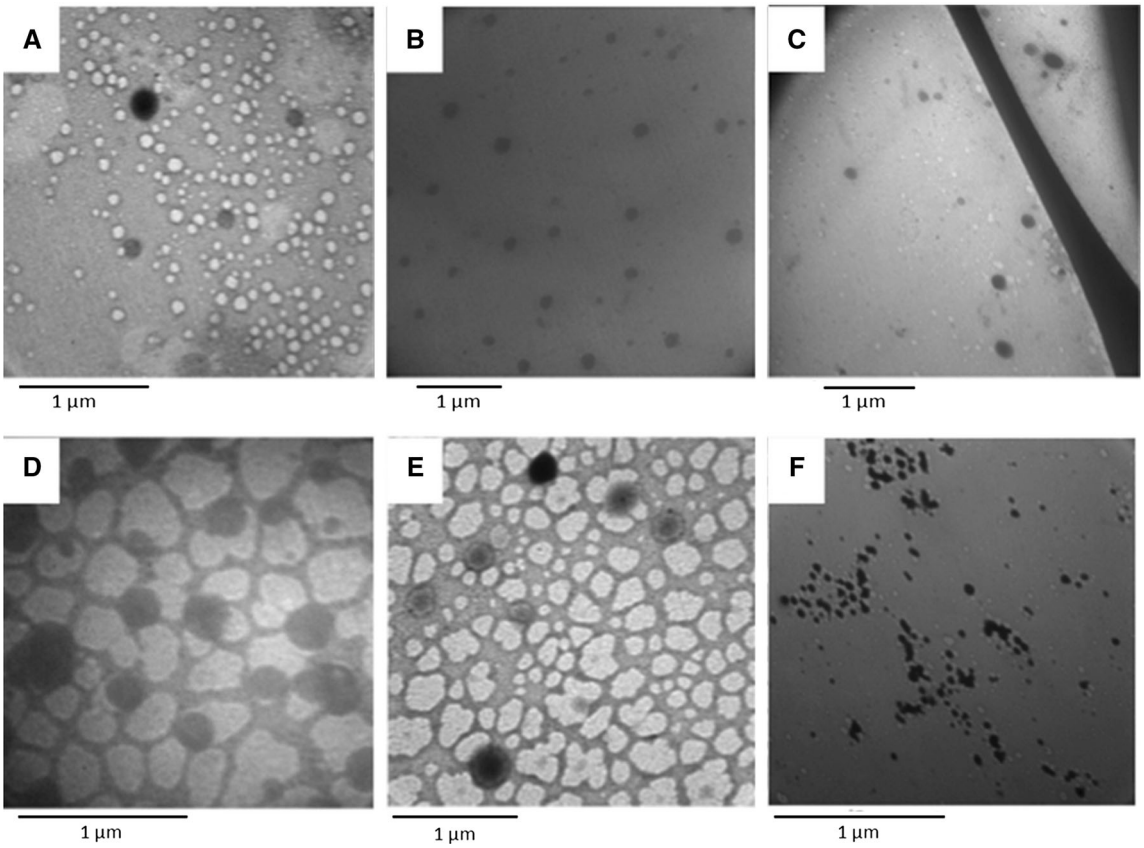

Fig. 1 Representative electron microscopy images of synthesized nanoparticles. The nanoparticles are dark grey. **a** Empty PHBV nanoparticles, **b** PHBV nanoparticles containing paclitaxel, **c** PHBV nanoparticles containing superparamagnetic iron oxide nanoparticles (SPIONs), **d** PHBV nanoparticles containing clarithromycin, **e** PHBV nanoparticles containing clarithromycin and paclitaxel, **f** PHBV nanoparticles containing SPIONs, clarithromycin and paclitaxel. Scale bar are 1 µm

interactions in different parts of the polymeric structure, decreasing competition for the binding sites of both drugs. It is possible that there is a greater amount of clarithromycin in the most amorphous fraction of the polymeric matrix and a greater of paclitaxel in the crystalline fraction, which would affect the release of both drugs by first facilitating the release of clarithromycin and then delaying the release of paclitaxel. To determine whether situation occurs, it is necessary to determine the simultaneous release profile of the drugs. Only the paclitaxel

Table 4 Efficiency of the encapsulation (%EE) of paclitaxel and clarithromycin in polymeric nanoparticles

Nanoparticle	%EE paclitaxel	%EE clarithromycin
E	0	0
T	48.5 ± 1.5	0
C	0	37.6 ± 6.2
CT	41.2 ± 6.3	36.1 ± 4.1
S	0	0
SC	0	33.0 ± 0.2
ST	44.1 ± 0,6	0
SCT	44.4 ± 1.3	32.6 ± 1.5

(E) Empty PHBV nanoparticles, (T) PHBV nanoparticles containing paclitaxel, (C) PHBV nanoparticles containing clarithromycin, (CT) PHBV nanoparticles containing clarithromycin and paclitaxel, (S) PHBV nanoparticles containing superparamagnetic iron oxide nanoparticles (SPIONs), (SC) PHBV nanoparticles containing SPIONs and clarithromycin, (ST) PHBV nanoparticles containing SPIONs and paclitaxel, and (SCT) PHBV nanoparticles containing SPIONs, clarithromycin and paclitaxel. Data were presented as mean ± SD (n = 3)

release profile was analyzed (Fig. 3), because we doṅt need high levels of free paclitaxel during the first hours of treatment, to reduce its toxic effects on healthy tissues. This concept is key to prove that encapsulation of paclitaxel in PHBV nanoparticles reduces its toxic effects present in its conventional pharmaceutical form, a problem that does not have clarithromycin. At 28 h, a release percentage of 0.7% paclitaxel was determined from T nanoparticles and 1.8% from ST nanoparticles. As expected, no paclitaxel release from the control E nanoparticles (empty nanoparticles) was detected.

The bioactivity of encapsulated clarithromycin against Neisseria gonorrhoeae (Ngo) was analyzed by Kirby-Bauer test to determine whether the antibiotic maintained its antimicrobial activity after the synthesis protocol. The Fig. 4a, b show that encapsulated clarithromycin has similar diameter of inhibition halo (mm) compared to clarithromycin non-encapsulated. This result was expected because non-encapsulated clarithromycin levels in the control are similar to the clarithromycin encapsulated. The nanoparticles with clarithromycin was previously treated

A

Total interaction energy including the Van der Waals (VdW) and electrostatic energy components

	TOTAL (kcal/mol)		VdW (kcal/mol)		Electrostatic (kcal/mol)	
COMPLEXES	**Minimum**	**Average**	**Minimum**	**Average**	**Minimum**	**Average**
Paclitaxel - PHVB	-19.351	-3.460	-19.433	-3.458	-3.009	-0.002
Clarithromycin- PHVB	-17.912	-3.516	-17.801	-3.516	-2.836	-0.001
Paclitaxel - Paclitaxel	-20.481	-3.163	-20.725	-3.164	-2.729	0.001
Clarithromycin-Clarithromycin	-15.231	-3.070	-15.280	-3.071	-3.111	0.001

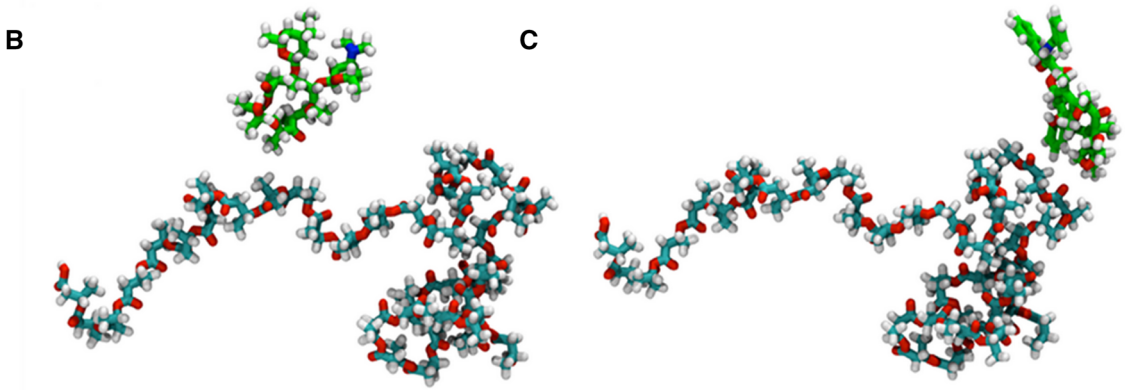

Fig. 2 Minimum energy conformation between drugs and polymers. **a** The table with total interaction energy including the Van der Waals (VdW) and electrostatic energy components. **b** The minimum energy conformation between clarithromycin and PHBV. **c** The minimum energy conformation between paclitaxel and PHBV

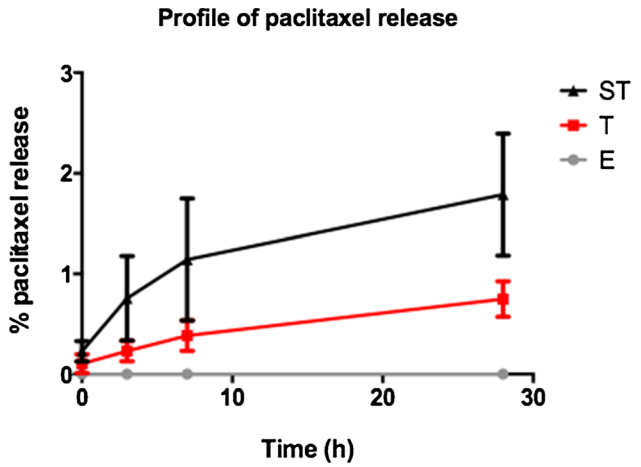

Fig. 3 Profile of paclitaxel release from PHBV nanoparticles. Percentage of paclitaxel released at different time from nanoparticles E (empty), T (with paclitaxel) and ST (with SPIONs and paclitaxel). Data were presented as mean ± SD (n = 3)

with dichloromethane for release all encapsulated antibiotic. Finally, to determine the in vitro toxicity of all PHBV nanoparticles synthesized an in vitro toxicology tests on cell viability of Eahy.926 cells were carried out, Fig. 4c. These results show that all the evaluated nanoparticles had an IC 50 above 100 mg/ml. These results indicate that all PHBV nanoparticles synthesized can be administered through an intravenous bolus, without being toxic to the vascular endothelium.

Discussion

The present study shown that only modifying the paclitaxel solvent, we improve the solubility of the drug and increasing the encapsulation area, which improved the encapsulation efficiency to 48.53%. These nanospheres

A

Treatment	Diameter of inhibition halo (mm)
Clarithromycin	27 ± 6
E	0 ± 0.0
C	13 ± 6
CS	16 ± 9
CT	11 ± 3
SCT	11 ± 1

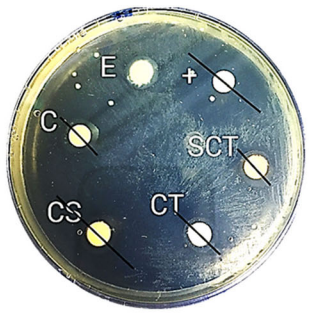

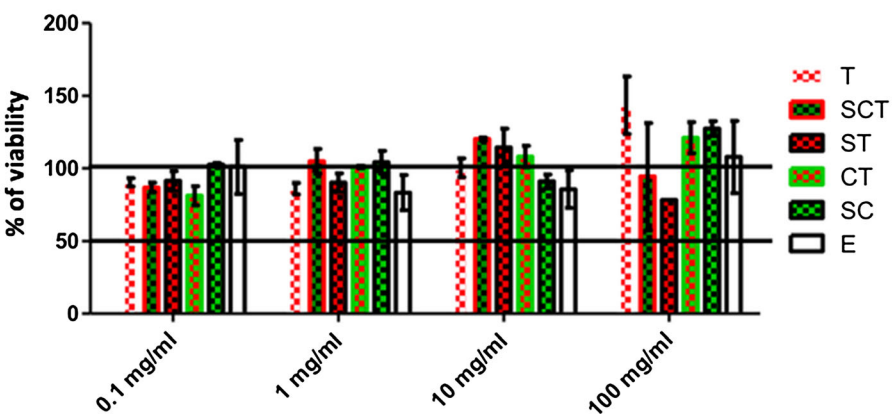

Fig. 4 The bioactivity of encapsulated clarithromycin and In Vitro toxicology tests of all PHBV nanoparticles synthesized. **a** The table shows Kirby-Bauer test against Ngo by the inhibition halos diameter. The positive (+) control consisted of 10 µg of unencapsulated clarithromycin. For each sensidisc, 4 mg of lyophilized nanoparticles was used. (E) Empty PHBV nanoparticles, (C) PHBV nanoparticles with clarithromycin, (CS) PHBV nanoparticles with clarithromycin and superparamagnetic iron oxide nanoparticles (SPIONs), (CT) PHBV nanoparticles with clarithromycin and paclitaxel and (SCT) PHBV nanoparticles with clarithromycin, SPIONs and paclitaxel. Data were presented as mean ± SD (n = 3). **b** The figure shows an antibiogram representative image. **c** The graph shows the effect of PHBV nanoparticles on cell viability of Eahy.926 cells. Cells viability was measured by absorbance analysis with 4 different concentrations of nanoparticles. (T) PHBV nanoparticles with paclitaxel, (SCT) PHBV nanoparticles with SPION, clarithromycin and paclitaxel, (ST) PHBV nanoparticles with SPION and paclitaxel, (CT) PHBV nanoparticles with clarithromycin and paclitaxel, (SC) PHBV nanoparticles with SPION and clarithromycin, and (E) empty nanoparticles. Data were presented as mean ± SD (n = 3)

were synthesized using DMSO as a solvent for the PHBV polymer and for paclitaxel, because paclitaxel is a highly hydrophobic, it does not have good solubility in aqueous solutions. With this modification, nanospheres were synthesized instead of nanocapsules, compared to previous studies that show nanocapsules synthesized using aqueous solution as a solvent for paclitaxel and DMSO for the PHBV polymer. These results are according with previous studies that show that our protocol is capable of encapsulating and maintaining paclitaxel activity, with encapsulation efficiency over 37.25% [25].

All the nanoparticles obtained had a size between 190 and 230 nm, with a single hydrodynamic diameter compatible with spherical nanoparticles (Tables 1 and 3), as verified by electron microscopy (Fig. 1). The nanoparticles had a negative Z potential (Tables 1 and 3) and were hydrophilic (Table 2), allowing their use in living organisms [30]. Nanoparticles with these characteristics should have low toxicity and a high half-life in blood, having all the necessary characteristics for EPR and intravenous injection [30]. Taking into account the physicochemical characteristics of all the nanoparticles obtained, it is expected that they will have a high half-life in the bloodstream [30–32] and that they will be passively located in areas with a high blood supply and permeability [30]. This type of microenvironment is typical of carcinomas where angiogenesis is relevant, so it is expected that these nanoparticles will accumulate in the microenvironments of tumor masses, which makes then excellent vehicles for antineoplastic drugs. On the other hand, nanoparticles that contain SPIONs can be actively directed through the use of a magnetic field. Therefore, the dose of drugs to be used against lung cancer should be recalculated to reach a therapeutic dose only in that organ [10]. On the other hand, the hydrophilicity of the synthesized nanoparticles allows their solubilization and administration in physiological serum or other polar vehicles, which is an advantage over commercial paclitaxel, which is administered with polyethoxy castor oil and dehydrated alcohol. Polyethoxylated castor oil is related to several hypersensitivity reactions, such as anaphylaxis, dyspnea, hypotension, angioedema, and generalized urticaria; fatal reactions to castor oil have even occurred despite the administration of a medication that decreases these hypersensitivity reactions [33]. These reactions are why all patients should be pretreated with corticosteroids (e.g., dexamethasone), diphenhydramine (H1 antagonist), and H2 antagonists (e.g., cimetidine or ranitidine), as H2 receptors are related to hypotension symptoms and secondary edema [34]. The development of a pharmaceutical form of paclitaxel that allows avoidance of the use of an excipient will have a great impact reducing these side effects. On the other hand, the PHBV polymer used in this new pharmaceutical form is biodegradable and biocompatible. In addition, PHBV is non-toxic, has high compatibility with a large number of cell lines and can be produced on a large scale [27, 35, 36].

Finally, SPIONs are highly biodegradable, since they can be dissociated into iron and oxygen within the body and safely eliminated using the metabolism and oxygen transport system [37, 38]. Iron released from SPIONs is metabolized by the liver and subsequently used in the formation of red blood cells or excreted via the kidney [39].

As the synthesized nanoparticles had the desired behavior, their %EE, component activity and the molecular interactions between them were evaluated. Although all the biologically active components of the nanoparticles were hydrophobic, encapsulation of more than one component at a time had little effect on the %EE of paclitaxel. This may be because, as shown in Fig. 2, paclitaxel and clarithromycin interact differently with the PHBV polymer in their lowest energy conformation, limiting competition between the two drugs. According with the molecular modeling results is possible that paclitaxel mostly interacts in the crystalline phases of the polymer in the nanoparticles and that clarithromycin mostly interacts with the amorphous phases, affecting its release profile as well as the ratio of both phases, which would be interesting to evaluate by means of a calorimetry test. The ratio between the amorphous phase and the crystalline phase of the polymer has a strong impact on the dissolution and release of the drugs, as well as on the absorption of the active principles by the organism. If we compare the amorphous phase with the crystalline phase of a polymer, the compaction of the amorphous phase is less than the crystalline phase, with spaces between the polymer chains. These spaces favor the entry of water between the polymeric matrix, increasing the speed of liberation and dissolution of drugs. The molecular modeling results show that clarithromycin is preferably found in the amorphous phases of the polymer, while paclitaxel is preferably found in the more crystalline phases. These localization impact the release profiles of these drugs, as it is expected that the rate of release of clarithromycin from the polymeric matrix is higher than the rate of release of paclitaxel and that, in addition to being simultaneously encapsulated within a polymeric nanoparticle, paclitaxel is released faster than when it is encapsulated alone. This situation was partly demonstrated by analyzing the release profile of paclitaxel from polymer nanoparticles when encapsulated along (T) or accompanied by SPIONs (ST) (Fig. 3). As observed from, paclitaxel is released more quickly when encapsulated in PHBV nanoparticles in conjunction with SPIONs. The only difference between the two nanoparticles is the addition of SPIONs to the polymer matrix, which increases the amount of amorphous phase of the polymer, facilitating the entry of

water and the dissolution and subsequent release of paclitaxel from the PHBV nanoparticles. Previous results showed that PHBV nanoparticles have an increased volume in aqueous solutions at pH 7.4 [25].

Interestingly the bioactivity of encapsulated clarithromycin, antimicrobial activity, was similar compared to clarithromycin non-encapsulated. Finally the in vitro toxicity of the synthesized nanoparticles was quantified, and an IC50 greater than 100 mg/ml was found in Eahy.926 endothelial cells. This results was expected, because in the first 28 h only 0.7% of paclitaxel was released while that the 99,3% of paclitaxel remains encapsulated and non-bioavailable. Since the synthesized nanoparticles have been designed and selected to be administered through an intravenous bolus, it was of enormous importance to quantify the cytotoxicity of these nanoparticles in this cell type.

Conclusion

PHBV polymer nanoparticles can be used as hydrophilic vehicles for hydrophobic drugs with different physicochemical properties, such as antineoplastic paclitaxel, macrolide clarithromycin and SPIONs. None of these compounds lose their biological activity and all would be candidates for use in the theranostics of lung cancer or other type cancer associated with bacterial infections.

Acknowledgements We thank the CONICYT—PCHA/ Doctorado nacional/ 2013-21130869, and SEK University SEK1905.

Authors' Contributions PS and MG contributed to the conception of the work, designing experimental methodologies, conducted experiments and helped in writing the manuscript. FGN conducted experiments of molecular modeling. DC, NH, NJ, SD and MM contributed statistics, table design and image analysis. PS, MG and IB conducted to the In vitro toxicity assay. SH contributed to writing and approving the final form of the manuscript. LV contributed to the conception of the work, interpretation of the results and approving the final form of the manuscript. All authors read and approved the final manuscript.

Funding This work was supported by CONICYT—PCHA/ Doctorado nacional/2013–21130869, and SEK University, SEK1905.

Availability of Data and Materials Not applicable.

Compliance with Ethical Standards

Ethics Approval Not applicable.

Conflict of interest All authors declare no conflict of interest.

References

1. Bray F, Ferlay J, Soerjomataram I, Siegel RL, Torre LA, Jemal A, CA Cancer J Clin. 68, 394-424 (2018)
2. Philip R; Williams JP, Oncologia Clínica, 8va ed. (Elsevier, España, 2003), pag. 823
3. Kreuzer M, Heinrich J, Kreienbrock L, Rosario AS, Gerken M, Wichmann HE, Int J Cancer. 100, 706-13 (2002)
4. Su X, Li G, Hai Z, Yang H, Hunan Yi Ke Da Xue Xue Bao. 23, 76-8 (1998)
5. Hammerschlag MR, Qumei KK, Roblin PM, Antimicrob Agents Chemother. 36, 1573-4 (1992)
6. Bhatia S. Natural polymer drug delivery systems. Berlin: Springer; 2016, p. 225
7. Wadajkar AS, Menon JU, Kadapure T, Tran RT, Yang J, Nguyen KT, Recent Pat Biomed Eng. 6, 47-57 (2013)
8. Veiseh O, Gunn JW, Zhang M, Adv Drug Deliv Rev. 62, 284-304 (2010)
9. Xie J, Lee S, Chen X, Adv Drug Deliv Rev. 62, 1064-79 (2010)
10. Gupta AK, Naregalkar RR, Vaidya VD, Gupta M, Nanomedicine (Lond). 2, 23-39 (2007)
11. Vilos C, Gutierrez M, Escobar RA, Morales F, Denardin J, Velásquez L, Altbir D, Electronic Journal of Biotechnology. 16, 1-10 (2013)
12. Kohler N, Sun C, Fichtenholtz A, Gunn J, Fang C, Zhang M, Small. 2, 785-92 (2009)
13. Hayashi K, Nakamura M, Sakamoto W, Yogo T, Miki H, Ozaki S, Abe M, Matsumoto T, Ishimura K, Theranostics. 3, 366-76 (2013)
14. Wust P, Hildebrandt B, Sreenivasa G, Rau B, Gellermann J, Riess H, Felix R, Schlag PM Lancet Oncol. 3, 487-97 (2002)
15. Silva AC, Oliveira TR, Mamani JB, Malheiros SM, Malavolta L, Pavon LF, Sibov TT, Amaro E Jr, Tannús A, Vidoto EL, Martins MJ, Santos RS, Gamarra LF, Int J Nanomedicine. 6, 591-603 (2011)
16. Torchilin VP, Adv Drug Deliv Rev. 58, 1532-55 (2006)
17. Sun C, Lee JS, Zhang M, Adv Drug Deliv Rev. 60, 1252-65 (2008)
18. Yu MK, Jeong YY, Park J, Park S, Kim JW, Min JJ, Kim K, Jon S, Angew Chem Int Ed Engl. 47, 5362-5 (2008)
19. Yang J, Lee CH, Ko HJ, Suh JS, Yoon HG, Lee K, Huh YM, Haam S. Multifunctional magneto-polymeric nanohybrids for targeted detection and synergistic therapeutic effects on breast cancer. Angew Chem Int Ed Engl. 2007;46:8836-9.
20. Lin JJ, Chen JS, Huang SJ, Ko JH, Wang YM, Chen TL, Wang LF, Biomaterials. 30, 5114-24 (2009)
21. Kaaki K, Hervé-Aubert K, Chiper M, Shkilnyy A, Soucé M, Benoit R, Paillard A, Dubois P, Saboungi ML, Chourpa I, Langmuir. 28, 1496-505 (2012)
22. Kievit FM, Stephen ZR, Veiseh O, Arami H, Wang T, Lai VP, Park JO, Ellenbogen RG, Disis ML, Zhang M, ACS Nano. 6, 2591-601 (2012)
23. Parker JS, Mullins M, Cheang MC, Leung S, Voduc D, Vickery T, Davies S, Fauron C, He X, et al, J Clin Oncol. 27, 1160-7 (2009)
24. Solar P, González G, Vilos C, Herrera N, Juica N, Moreno M, Simon F, Velásquez L, J Nanobiotechnology. 13, 1-12 (2015)
25. Vilos C, Morales FA, Solar PA, Herrera NS, Gonzalez-Nilo FD, Aguayo DA, Mendoza HL, Comer J, Bravo ML, Gonzalez PA, Kato S, Cuello MA, Alonso C, Bravo EJ, Bustamante EI, Owen GI, Velasquez LA, Biomaterials. 34, 4098-4108 (2013b)
26. Mao S, Xu J, Cai C, Germershaus O, Schaper A, Kissel T, Int J Pharm. 334, 137-48 (2007)
27. Schnoor B, Elhendawy A, Joseph S, Salvador-Morales C, Journal of Agricultural and Food Chemistry. 66, 1-15 (2018)

28. McNeil SE, Wiley Interdiscip Rev Nanomed Nanobiotechnol. 1, 264-71 (2009)
29. Tadmor R, Langmuir. 20, 7659-64 (2004)
30. Nel AE, Mädler L, Velegol D, Xia T, Hoek EM, Somasundaran P, Klaessig F, Castranova V, Thompson M, Nat Mater. 8, 543-57 (2009)
31. Maeda H, Nakamura H, Fang J, Adv Drug Deliv Rev. 65, 71-9 (2013)
32. Torchilin V, Adv Drug Deliv Rev. 63, 131-5 (2011)
33. Wang H, Cheng G, Du Y, Ye L, Chen W, Zhang L, Wang T, Tian J, Fu F, Mol Med Rep. 7, 947-52 (2013)
34. yPiccart MJ, Klijn J, Paridaens R, Nooij M, Mauriac L, Coleman R, Bontenbal M, Awada A, Selleslags J, Van Vreckem A, Van Glabbeke M, J Clin Oncol. 15, 3149-55 (1997)
35. Wang L, Du J, Cao D, Wang Y, Journal of Macromolecular Science Part A. 50, 885–893 (2013)
36. Chang HM, Wang ZH, Luo HN, Xu M, Ren XY, Zheng GX, et al, Brazilian Journal of Medical and Biological Research. 47, 533–539 (2014)
37. Dobson J, Gene therapy. 13, 283-287 (2006)
38. Gupta AK. and Wells S. IEEE transactions on nanobioscience. 3, 66-73 (2004)
39. Anzai Y, Piccoli CW, Outwater EK, Stanford W, Bluemke DA, Nurenberg P, Saini S, et al, Radiology. 228, 777-788 (2003)